IEEE Access
Multidisciplinary | Rapid Review | Open Access Journal

Received January 7, 2021, accepted January 19, 2021, date of publication January 25, 2021, date of current version February 1, 2021.

Digital Object Identifier 10.1109/ACCESS.2021.3054389

Calibration and Equalization for the Measurement Channels of a Photoelectric Testing System With Intersecting Detection Areas

DING CHEN[1,2], (Member, IEEE), AND JINPING NI[2]
[1]School of Armament Science & Technology, Xi'an Technological University, Xi'an 710021, China
[2]Shaanxi Province Key Laboratory of Photoelectric Measurement and Instrument Technology, Xi'an Technological University, Xi'an 710021, China

Corresponding author: Ding Chen (chending@xatu.edu.cn)

This work was supported in part by the Natural Science Foundation of Shaanxi Province of China under Grant 2019JM-601 and in part by the Scientific Research Programming Project of Shaanxi Provincial Education Department under Grant 20JK0692.

ABSTRACT There are usually non-equilibrium transmission characteristic among the measurement channels of a photoelectric testing system with intersecting detection areas, and it will lead to a poorer measurement result provided that they are not properly calibrated and equalized. To improve the measurement accuracy of the system, this article presents an original calibration & equalization method to effectively restrain the effect of the non-equilibrium transmission characteristics. The measurement principle of this system is described in detail. Then, main transmission characteristic of the measurement channel is analyzed, and a calibration model is established and the requirements of its calibration signal are considered. Next, the equalization principle of measurement channel is studied, and then a compensating network is developed to perform an iterated algorithm to equalize the measurement channels. Through semi-physical simulation, the results show that an experiment platform is developed to generate several parallel calibrated signals with quasi–delta, and this can obtain the key characteristic (i.e., delay time) of the measurement channels. Furthermore, the transmission delay difference between any two measurement channels is below 0.5μs through iterated equalization. Consequently, the proposed calibration and equalization method can effectively decrease the systematic error of the testing system.

INDEX TERMS Photoelectric testing system, multichannel, measurement accuracy, transmission delay, calibration, equalization.

I. INTRODUCTION

The motion parameters (i.e., instantaneous velocity, attitude angle, hit coordinates etc.) of some small flying targets, such as bullet, projectile, debris, sport ball and small unmanned aerial, attract much interest in various fields. In shooting range test, the damage effectiveness of small arms is mainly determined by its firing accuracy and bullet speed. During the training of some sport balls (e.g., baseball, golf ball, football, etc.), it can give some good advises for athletes to improve their competitive performance if the flying velocity of the ball and its attitude angle are accurately known. For safe guarding, it is necessary that the velocity and flying direction of suspected small unmanned aerial near the protected facilities can be detected. Currently, there are some measurement methods based on different detection principles of high-speed photography [1]–[3], photoelectricity [4]–[6], acoustic [7] and [8], radar [9] and [10], double–CCD intersection [11] and [12]; wherein, a testing system with intersecting detection areas using passive photoelectric detection has many advantages of high detection sensitivity, high measure precision, greater range of velocity measurement, low maintenance cost, easily operating, and high reliability compared with other methods. Therefore, it has been widely used to measure the motion parameters of small flying target. With higher measurement requirement, it is necessary to improve its performance, especially measurement accuracy. According to its measurement theory, the measurement performance of this instrument is mainly affected by two factors. One factor is the key structural parameters (i.e., spatial structural relationship among its detection areas) of the system, and it is because that measurement model can be established on the basis of the above parameters; another one is the arrival time parameter when the measured target arrives at its detection area, and then this parameter as independent variable is substituted into the measurement model to

The associate editor coordinating the review of this manuscript and approving it for publication was Chao Tan.

obtain the above motion parameters. Therefore, they must be deeply taken into consideration to improve the measurement performance.

Until now, some investigations are carried out in the field. On the one hand, Z. Wu *et al*. designed a verification mechanism of the key structure parameters using the combination of several lasers. It can obtain the key structure parameters, thereby establishing more precise measurement model [13]. However, the mechanism is relatively complicated, particularly poor operability. R. Chen and J. Ni proposed a calibration platform of key structural parameters. Compared with previous methods, the method is simpler and easier; specially, the platform is automatically performed [14]. Unfortunately, measurement model is relatively poor if adopting this method. Furthermore, R. Chen *et al*. also put forward an inversion method of the key structure parameters using genetic algorithm. Through iterations, the most accurate key structural parameters can be obtained to build an optimized measurement model [15]. On the other hand, for the arrival time parameter, J. NI and H. TIAN put forward an approach of -3 dB amplitude along drop edge and a generalized correlation method to obtain the arrival time parameter from signal waveform. The former method can be only used under high signal-to-noise ratio (SNR) condition, but the latter method has good noise immunity [16] and [17]. Besides, author and his colleagues proposed an estimation method of the arrival time parameter using pulse compression. It can extract the arrival time parameter under poorer signal-to-noise ratio condition [18] and [19]. However, prior researches only focused on the two above aspects, and there is almost no research on a problem. Usually, there is the non-equilibrium transmission characteristic among multiple measurement channels, so this brings about a significant influence on the estimation of the arrival time parameter. Obviously, it is a very demanding application to calibrate and equalize the measurement channels. Increasingly higher measurement requirement further complicates this task. Fortunately, some new technologies also enable some more powerful methods. Therefore, we can realize the solution for the calibration and equalization.

In this research, we propose a method to calibrate and equalize the measurement channels in the photoelectric instrument. We describe the measurement principle in detail, and the transmission characteristic of its measurement channels is analyzed. Next, we develop an experiment platform to output the parallel signals with quasi–δ into their corresponding measurement channels according to the requirements of the calibration signal. This can effectively obtain the non-equilibrium characteristics among the measurement channels. Finally, we perform an equalization method through iteration. The experiment is also given to show the validity and feasibility of the proposed method, and thus it can avoid the influence from then non-equilibrium of the measurement channels on the estimation of the time parameter.

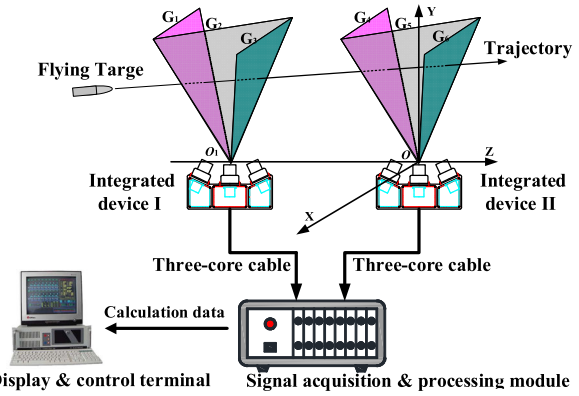

FIGURE 1. Schematic diagram of a typical photoelectric testing system with six intersection detection areas.

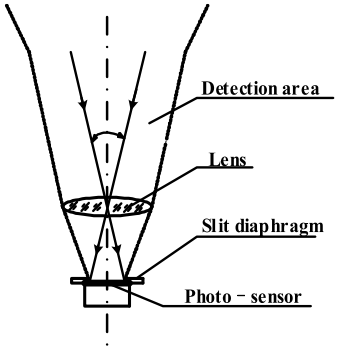

FIGURE 2. Design principle of the photo–detector.

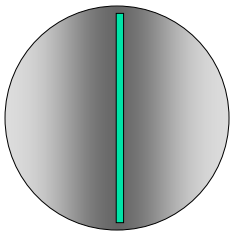

FIGURE 3. Schematic diagram of the slit diaphragm in the photo–detector.

II. MEASUREMENT PRINCIPLE

A. SYSTEM COMPOSITION

As shown in Fig.1, this is a typical photoelectric testing system with six intersection detection areas. Generally, it consists of several pairs of photo–detectors, a signal acquisition & processing module, a display & control terminal, and so forth; herein, the photo–detectors (see Fig.2) are the key part of the system. Specially, a slit diaphragm (see Fig.3) is installed beneath the lens of the photo–sensor. Consequently, its field of view can be limited to form a fan-shaped detection area with thinner thickness (usually, less than 1mm), and thus it is also called light curtain. Considering compact structure, three photo–detectors are generally assembled together in an integrated device. Typically, there are a pair of the integrated devices, namely six photo–detectors in the system.

When a flying target passes through a light curtain, the luminous flux of the lens is shaded partly by it, and then

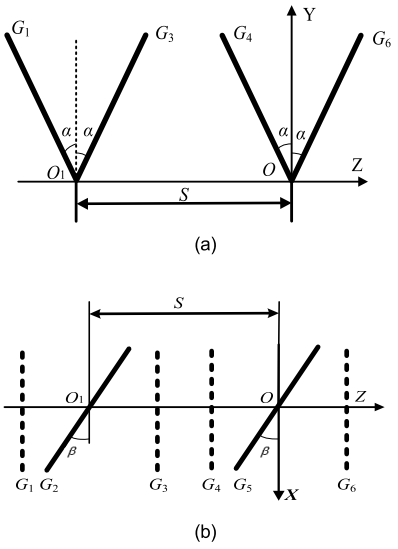

FIGURE 4. Projection view of the six light curtains on the two planes, (a) projection view on YOZ–plane, (b) projection view on ZOX–plane.

this leads to a momentary decline in the output current of the corresponding photo–detector. Through the signal processing circuit, the changing current is converted into a pulse signal. Likewise, if a flying target passes through the six light curtains, which are denoted as G_1, G_2, G_3, …, G_6, respectively, six pulse signals will be generated to output into the signal acquisition & processing module. In the module, six arrival time parameters (i.e., t_1, t_2, t_3, …, t_6) can be extracted from these six pulse signals according to some algorithms [16] – [19]. According to the measurement model, these arrival time parameters are used to calculate the measurement results, including instantaneous velocity, attitude angle, hit coordinates, and then these calculation data are displayed on the display & control terminal. Even if these photo–detectors are made using the same type components, they cannot be consistent in electrical characteristics.

B. MEASUREMENT MODEL

Supposing that these six light curtains are located in a Cartesian coordinate system in Fig.1. The original point O of this coordinate system is an intersection point of the light curtain G_4, G_5 and G_6. The OZ is the direction of an intended trajectory, and the direction of OY is upward; in addition, the OX is perpendicular to the OY. Consequently, the three axes form a left-hand coordinate system. To further illustrate the spatial structural relationships among the six light curtains, they are projected on the ZOX–plane and the YOZ–plane as shown in Fig.4 (a) and (b). Obviously, there are three key structure parameters including S, α and β. The parameter of S is the range between the two points of O and O_1; specially, the point O_1 is an intersection point of the light curtain G_1, G_2 and G_3. In Fig.4 (a), the parameter of α is the intersection angle between the light curtain G_4 and the XOY–plane (called measurement plane), and the two-light curtain G_4 and G_5 are symmetrically arranged at both sides of the XOY–plane. Besides, the two-light curtain G_1 and G_4 are parallel to each other, and there is also a parallel relationship between the two-light curtain G_3 and G_6. In Fig.4 (b), the parameter of β is the intersection angle between the light curtain G_5 and the target face, and the two-light curtain G_2 and G_5 are parallel to each other. Despite the above key

structural parameters are identical with designed values as far as possible, there are a few of deviations between them in engineering. Evidently, this will lead to an inaccurate measurement model. In the research, we make the assumption that the optical structure of the system is properly calibrated and adjusted, and then an accurate measurement model can be obtained according to these key structural parameters. Therefore, effects of the key structural parameters can be ignored

In [20], it has been discussed how to establish the measurement model in detail. In this Section, we give the matrix form of the measurement model directly, as follows.

$$\boldsymbol{X} = \boldsymbol{M}^{-1} \cdot \boldsymbol{N} \tag{1}$$

with

$$\boldsymbol{M} = \begin{bmatrix} \cos\alpha & -\sin\alpha & 0 & \cos\alpha \cdot t_3 & -\sin\alpha \cdot t_3 & 0 \\ \cos\beta & 0 & \sin\beta & \cos\beta \cdot t_2 & 0 & \sin\beta \cdot t_2 \\ \cos\alpha & \sin\alpha & 0 & 0 & 0 & 0 \\ \cos\alpha & -\sin\alpha & 0 & \cos\alpha \cdot t_6 & -\sin\alpha \cdot t_6 & 0 \\ \cos\beta & 0 & \sin\beta_2 & \cos\beta \cdot t_5 & 0 & \sin\beta \cdot t_5 \\ \cos\alpha & \sin\alpha & 0 & \cos\alpha \cdot t_4 & \sin\alpha \cdot t_4 & 0 \end{bmatrix},$$

$$\mathbf{X} = \begin{bmatrix} x \\ y \\ z \\ v_x \\ v_y \\ v_z \end{bmatrix} \text{ and } \boldsymbol{N} = \begin{bmatrix} 0 \\ 0 \\ 0 \\ -S\cos\alpha \\ -S\cos\beta \\ -S\cos\alpha \end{bmatrix} \text{ where } x, y \text{ and } x$$

are the hit coordinate on the target face, v_x, v_y and v_x are the decomposition of flight velocity along the three axes of X, Y and Z. t_1, t_2, t_3,…, t_6 are the time when the projectile arrives at the light curtain G_1, G_2, G_3, …, G_6, respectively, S, α and β are the key structure parameters of the system.

Note that these time parameters are not absolute time. Usually, the first-time arrival time parameter t_1 is deemed to be starting time and it is set to 0. Accordingly, other arrival time parameters (i.e., t_2, t_3, t_3, …, t_6) are time interval relative to t_1. As an independent variable, the arrival time parameter dominates the measurement results of the flying target based on the accurate measurement model. In engineering, the estimation of the arrival time parameter is seriously affected by plenty of random noise, such as sky background noise, electrostatic coupling noise, magnetic coupling noise, recombination noise and internal thermal noise. To restrain noise and against disturbing, there are all kinds of filters in the circuit of the system. Unfortunately, part of signal energy with the certain frequency spectrum is consumed notwithstanding most of the noise is filtered. It is inevitable that the distortion of the signal waveform occurs after filtering; particularly, multiple output signals in the channels are differently delayed. Hence this has an influence on the estimation of the arrival time parameter.

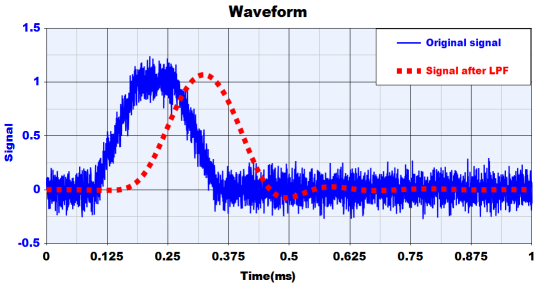

FIGURE 5. Signal after LPF vs original signal with noise in a measurement channel.

III. CALIBRATION METHOD

A. TRANSMISSION CHARACTERISTIC OF THE MEASUREMENT CHANNELS AND ITS CALIBRATION MODEL

In the system, there are six measurement channels which are corresponding to the six detection areas, respectively. The measurement channel mainly contains a photo–detector, a cable, connector and other auxiliaries. Because we adopt some cables and connectors with good features (i.e., low-loss, stable phase and electromagnetic shielding), they have little effect on the measurement channel; besides, its transmission distance is not long and only several meters. That is to say, the transmission characteristic of the measurement channel is only dominated by photo-detector. In the photo-detector, the purpose of signal processing can improve the signal quality, especially to filter out noise, and it includes photoelectric conversion, amplification, filtering, etc.

In the measurement channel, the low pass filter (LPF) is mainly performed to filter out noise. Generally, the lower its cut-off frequency is, the better its effect of filtering out noise. In theory, the effective bandwidth of pulse signal is the reciprocal of its time–width, and thus a narrow pulse has the wide frequency bandwidth. Especially, rising edge of the pulse signal and its trailing edge contain a large number of high frequency components. According to related algorithms [16] – [19], the Edge time is very important for the estimation on arrival time parameter. Unfortunately, high frequency component in the pulse signal is observably attenuated. As seen from the Fig.5, although the noise in the signal after LPF is removed relative to the original signal with noise, this also brings about the distortion of the pulse signal. Specially, the signal is delayed for a time. Furthermore, the electrical characters of these measurement channels are different, and then their transmission delay is not identical at all. In other words, the working bandwidth of every measurement channel becomes narrow due to LPF; besides, the working bandwidth after LPF are not same at all. This brings about the non-equilibrium of the measurement channels; thus, this has also the influence on the estimation of the arrival time parameter.

The block schematic diagram of a calibration model is shown in Fig.6, it can acquire the transmission characteristics of the measurement channel in their working bandwidth. Calibration signal source can generate a specific signal

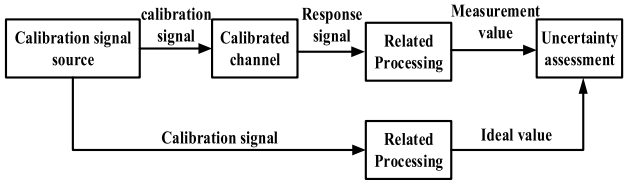

FIGURE 6. Block schematic diagram of a calibration model in a measurement channel.

(defined as calibration signal) with large bandwidth; especially, some key signal parameters, such as pulse width, edge time, amplitude, should be known. The calibration signal is then input into the calibrated channel. Consequently, almost intrinsic mode of these measurement channels can be effectively activated within their working bandwidth. At the same time, the calibrated channel generates a response signal. Some parameters (e.g., pulse width, edge time, amplitude, etc.) of the response signal can provide key evidence for the calibration. In the research, our biggest concern is the effect the arrival time parameter due to transmission characteristic. Therefore, measurement value is thus shown in the form of the arrival time parameter. However, the arrival time parameter cannot be directly obtained, and they can be calculated using some certain algorithms combined with some parameters of the response signal. Likewise, ideal value can be also calculated according to these key parameters of the calibration signal. Besides, note that this related processing is the estimation algorithm of the arrival time parameter in the model. By comparing ideal value with measurement value, we can obtain the transmission characteristic (mainly, transmission delay time) of the measurement channel. Finally, the calibration results are accurately achieved.

B. REQUIREMENTS OF THE CALIBRATION SIGNAL

In theory, a best calibration signal should be impulse signal due to its infinitely narrow time–width. Unfortunately, there is not this impulse signal or delta function signal in fact. According to [21], a signal with quasi–delta can be widely used to perform the calibration under a simulation environment. Generally, only high-performance signal source can generate the calibration signal whose parameters, such as pulse width, edge time, amplitude, are accurately configured in advance. These parameters can be used to calculate the ideal value, approximately.

When the projectile passing through the light curtain, the change curve of the luminous flux is a negative light pulse. Through signal processing, the photo-detector can output a positive pulse. They can be considered a pair of mirrored signals. To accurately obtain the transmission characteristic in the measurement channel, the calibration signal must simulate the change process of the luminous flux when the projectile passing through the light curtain. Therefore, the calibration signal should be also a negative light pulse, and its features must meet several requirements as follows. Firstly, its time-width should be as narrow as possible. This ensures the effective bandwidth of the calibration signal is wide enough so that it can fill over the pass-band of the

measurement channel. In this case, we can gain the most transmission characteristics because the high frequency component of the calibration signal is nearly attenuated. Secondly, because of several limitations in physics, the time-width of the calibration signal is not close to zero at all. Hence, its minimal time-width should meet the following requirement as below.

$$\tau_{\min} \geq \max(2T_s, \tau_o) \tag{2}$$

where $\tau_{\min}$ is the minimal time-width of the calibration signal, T_s is the sampling time, and τ_o is the response time of the photo-detector. Thirdly, the intensity of the calibration signal should be also proper. If it is too high, this leads to the saturation or breakdown of the photo-detector; conversely, the cut-off of the detector occurs. Besides, the light spectrum of the calibration signal must be in the detection range of the detector. Obviously, the accuracy of the calibration method is determined by the calibration signal, which must meet the above three requirements.

IV. EQUALIZATION METHOD

In theory, the aim of equalization is to expand the pass-band of a system as large as possible. This ensures that all frequency components of input signal can pass the equalized system without loss, so there is not almost the distortion of output signal relative to the input signal; meanwhile, the equalized system should also restrain noise, clutter and disturb in the input signal as far as possible. Through the ideal equalization, related information can be accurately extracted from the output signal due to high SNR.

Generally speaking, the output terminal of the equalized system is connected to a series module, which is defined as compensating network. Unfortunately, this cannot achieve the ideal equalization in engineering. In the equalized system, specific high frequency components within attenuation band are greatly attenuated using LPF; of course, most noise can be restrained at the same time. The purpose of the compensating network is to amplify the above attenuated signal within the attenuation band. Essentially, this compensating network is an especial amplifier with high gain. It is inevitable that a little noise, clutter and disturb enters the input of the compensating network again even if adopting interference shielding. Moreover, the compensating network amplifies the noise greatly. Obviously, it leads to the output signal with relatively poor SNR. Therefore, the traditional equalization method is not perfect.

A. PRINCIPLE OF THE EQUALIZATION METHOD

We make an assumption that six parallel calibration signals without noise entry their corresponding measurement channels of the calibrated channel, respectively. The six response signals with delay are outputted by these six measurement channels, respectively. Because of transmission characteristic differences among these measurement channels, their delay time are not identical at all, as depicted in Fig.7.

When a flying target passes through the six light curtains in turn, Their actual arrival time can be extracted using the

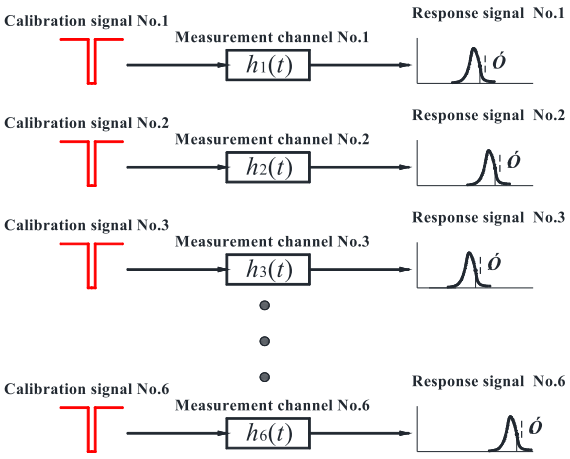

FIGURE 7. Schematic diagram of the response output signals affected by the transmission characteristic differences among the measurement channels.

method of −3 dB amplitude along drop edge. As was stated already, the arrival time parameters are really a series of time intervals relative to a certain reference time (i.e., t_1). The time t_1 when the flying target arrives at the first light curtain is be defined as a start time or reference time, and then it is set to 0. Based on the start time, the arrival time parameters are respectively expressed as

$$\begin{cases} t_1' = 0 \\ t_2' = t_2 + (\tau_2 - \tau_1) \\ t_3' = t_3 + (\tau_3 - \tau_1) \\ t_4' = t_4 + (\tau_4 - \tau_1) \\ t_5' = t_5 + (\tau_5 - \tau_1) \\ t_6' = t_6 + (\tau_6 - \tau_1) \end{cases} \tag{3}$$

with $\tau_1 \neq \tau_2 \neq \tau_3 \neq \tau_4 \neq \tau_5 \neq \tau_6$

where $t'_1, t'_2, t'_3, \ldots, t'_6$ are the actual arrival time parameters, $t_1, t_2, t_3, \ldots, t_6$ are the truth arrival time parameters, $\tau_1, \tau_2, \tau_3, \ldots, \tau_6$ are the transmission delay values of the six measurement channels, respectively. As can be seen from (3), the second term in the right side of each equation is a set of system errors, and they are time t caused by the transmission characteristic differences among the measurement channels.

If the measurement channels are connected in series with the compensating network with different transmission characteristics, respectively. After using the compensating networks, the transmission characteristics of the measurement channels are almost uniformity, as shown in Fig.8.

Considering the causality of the system, the delay time of the measurement channels cannot decrease through their compensating networks. For equalization, we should select a channel as the reference channel; specially, its delay time must be maximum in these measurement channels. Then, we suppose

$$\tau_{\max} = \max(\tau_1, \tau_2, \tau_3, \ldots, \tau_6) \tag{4}$$

The aim of equalization is that the delay time of every measurement channel becomes uniformity. In other words, the delay time of every measurement channel should be

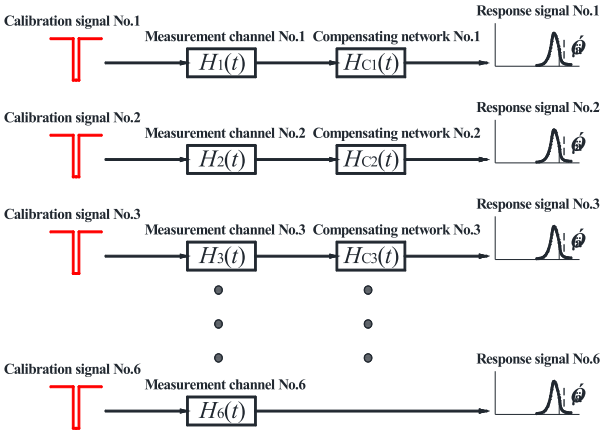

FIGURE 8. Schematic diagram of the response output signals through equalization.

that of the reference channel. Consequently, corresponding response signals should be parallel after parallel calibration signals enter their measurement channels. Through equalization, their delay time can be rewritten as

$$\tau_{\max} = \tau\prime_1 = \tau\prime_2 = \tau\prime_3 = \ldots = \tau\prime_6 (5) \tag{5}$$

where $\tau\ '_1, \tau\ '_2, \tau\ '_3, \ldots, \tau\ '_6$ are the transmission delay values of the six measurement channels through equalization, respectively. In Fig.7, supposing that the delay time of the sixth one is maximum in these measurement channels, and thus it is selected as the reference channel in Fig.8.

Likewise, the arrival time parameters can be also rewritten as

$$\begin{cases} t''_1 = 0 \\ t''_2 = t_2 + (\tau'_2 - \tau'_1) \\ t''_3 = t_3 + (\tau'_3 - \tau'_1) \\ t''_4 = t_4 + (\tau'_4 - \tau'_1) \\ t''_5 = t_5 + (\tau'_5 - \tau'_1) \\ t''_6 = t_6 + (\tau_6 - \tau'_1) \end{cases} \tag{6}$$

with $\tau\ '_1 = \tau\ '_2 = \tau\ '_3 = \tau\ '_4 = \tau\ '_5 = \tau\ '_6 = \tau_{\max}$

where $t''_1, t''_2, t''_3, \ldots, t''_6$ are the actual arrival time parameters through equalization, $t_1, t_2, t_3, \ldots, t_6$ are the truth arrival time parameters.

Obviously, Equations (1) can be derived as

$$\begin{cases} t''_1 = 0 \\ t''_2 = t_2 \\ t''_3 = t_3 \\ t''_4 = t_4 \\ t''_5 = t_5 \\ t''_6 = t_6 \end{cases} \tag{7}$$

As can be seen from (7), these measurement channels through equalization have no influence on the measurement accuracy in theory.

B. EQUALIZATION MODEL

Generally, traditional methods need to obtain the inverse system of compensated channel to build an ideal all-pass system.

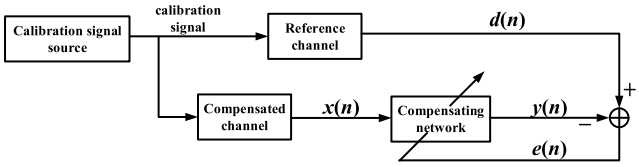

FIGURE 9. Schematic diagram of the equalization model based on iteration.

In fact, it is difficult to accurately obtain the transfer function of the compensated channel and its inverse system. As mentioned above, the compensated channel does not need to connect into its inverse system. In the research, we establish an equalization model as shown in Fig.9. In the model, an adaptive compensating network is connected to output of the compensated channel. After a calibration signal enters the reference channel, we can parameter through related processing. The arrival times parameter of the reference channel is deemed as an expectation value. Meanwhile, the calibration signal also enters the compensated channel, and then its arrival time parameter is also obtained; specially, this parameter is defined as the compensated value. Obviously, there is the error between the expectation value and compensated value. According to the error, the adaptive compensating network is reasonably adjusted. Through iterations, the error is decreased gradually. The iterative process may be continued until some criterion for convergence is met. In related technical requirements [22], they require that the difference of transmission delay between any two measurement channels is less than 5μs. Except for the difference of transmission delay, other factors should also be taken into consideration. According to error budget principles [23], the error is determined as 0.5μs.

In the research, the compensating network can be achieved through a classical adaptive traversal filter with N taps. We assume that the input vector of the compensating network is $\mathbf{x}(n)$, the coefficient vector of N tap weights is $\boldsymbol{w}(n)$ and the output vector of the compensating network is defined as

$$\begin{aligned} & y(n) = \boldsymbol{w}^T(n)\boldsymbol{x}(n) \\ \text{with} \quad & \boldsymbol{w}(n) = [w_0(n)w_1(n)\ldots w_{N-1}(n)] \\ \text{and} \quad & \boldsymbol{x}(n) = [x(n)x(n-1)\ldots, x(n-N+1)]^T \end{aligned} \tag{8}$$

where x(n) is also the output vector of the compensated channel, n is the word length of the proposed filter

In the model, the output of the reference channel is d(n), and it is defined as an expected value. The difference between d(n) and y(n) is defined as the error e(n), and it is expressed by

$$e(n) = d(n) - y(n) \tag{9}$$

According to Least Mean Square (LMS) algorithm, the coefficients vector of N tap weights is continuously adjusted, and the newer coefficients vector of N tap weights can be expressed by

$$\boldsymbol{w}(n+1) = \boldsymbol{w}(n) + 2\lambda e(n)\boldsymbol{x}(n) \tag{10}$$

where λ is the step - size of the lms algorithm

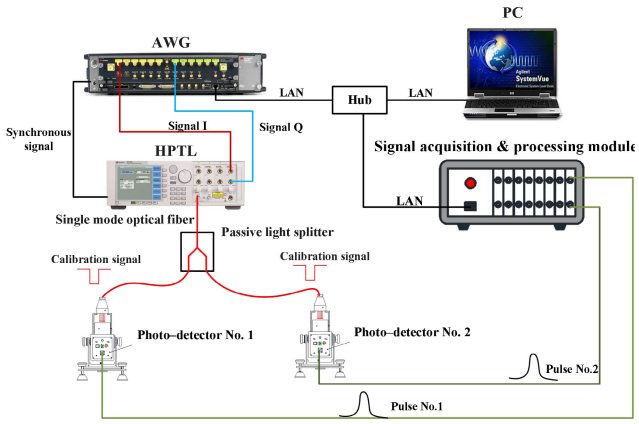

FIGURE 10. Block diagram of the calibration experiment platform.

TABLE 1. Main Specifications of the AWG

Parameter	Index
Sampling rate	Up to 65GSa/s
Analog bandwidth	8 bits
Digital-to-analog converter resolution	DC to 20GHz
Amplitude	-1.0V to +3.3V
Amplitude resolution	400μV
Edge time (Rise/fall time)	Down to 18ps
Time deviation	±6ps

Substituting (10) into (8), the newer output vector of the compensating network is calculated. Next, the newer error is obtained again. When the error reaches the minimum under the condition of mean square, the coefficients of tap weights are considered optimal. Finally, the compensated channel is approximately adjusted to the reference channel.

V. RESULTS AND DISCUSSION

A. EXPERIMENT PLATFORM

For convenience, we take the calibration for a system with only two measurement channels as for example, and it is usually called velocity testing system based on dual-light curtain. As shown in Fig.10, an experiment platform consists of an arbitrary waveform generator (AWG), a high-power tun-able laser (HPTL), a passive light splitter, a PC with waveform editing software, the two measurement channels and others. Hence, these instruments and their calibrated object form a closed loop system based on semi-physical simulation. The experiments, including calibration and equalization, should be performed in an ideal indoor environment because this can avoid the influence of the environmental noise as far as possible.

In the platform, an AWG of Keysight M8195A is adopted as the key component, and it has a series of merits as listed in Table 1. For the requirement of the calibration signal in (2), its time–width should be set to 0.4μs according to the above-mentioned calculation. Besides, its edge time is set to 18ps to obtain the optimal calibration signal; specially, this is the minimal edge time of signal generated from the AWG. According to some function definitions, customized wave-forms can be generated through a waveform edition software (i.e., Keysight SystemVue or Pulse Building). Using the waveform edition software in the PC, the initial waveform file of the calibration signal with quasi–delta can be compiled and downloaded into the AWG via LAN, independently. Due to the excellent performances of the AWG, all kinds of parameters of the calibration signal are accurate; specially, its time–width is extremely narrow (down to 50ps). In the AWG, built - in calibration equipment for frequency and phase is used to ensure the generated signal with little phase jitter. That is to say, its phase noise can be ignored.

Specially, the calibration signal is an optical signal not an electrical signal. In the platform, we use a HPTL of Keysight 81602A combined with the above AWG. The AWG can generate the two signals of I and Q and transmit into the HPTL, and then it can generate the calibration signal with quasi-delta through coherent modulation. For the photo-detector, the wavelength of this laser light should be in the visible spectrum. Consequently, the photo-detector can be effectively detect this calibration signal with quasi-delta. In addition, we must take into account coupler loss and insertion loss among photoelectric components of the platform. For our adopted HPTL, its relative noise intensity is below -150dB/Hz, and its side-mode suppression ratio is beyond 70dB. Therefore, the calibration signal can meet the requirement of the operation.

For the calibrated channel with two measurement channels, it is necessary that two calibration signals with quasi–delta are generated to calibrate it in the platform. Unfortunately, the high-power tun-able laser cannot meet the above requirement due to single generated signal. Therefore, we can use a passive light splitter to split a calibration signal into two ones. Note that the intensity of these two calibration signals will be severely attenuated through beam splitting. Before calibration, the intensity of the calibration signal is thus strong enough to equalize the coupler loss and insertion loss; otherwise, a very weak calibration signal will lead to the cut-off of photo-sensor in the photo-detector. If necessary, we can also add an amplifier into the output terminal of the HPTL before beam splitting. Of course, its intensity be appropriate in order that the photo-sensor is under the condition of linear amplification; specially, it must ensure the photo-sensor cannot be burnt.

Usually, there is a passive light splitter with one input terminal and eight output terminals not a passive light splitter with an input terminal and six output terminals in engineering. When the six output terminals are occupied, the remaining two output terminals should be also properly disposed. This can effectively avoid reflected light to enter the laser source again. In the research, a passive light splitter with one input terminal and two output terminals can meet the requirement.

For the calibration, there are no special requirements except intensity and delay. We can adopt single mode optical fiber with the length of two meters, and thus the transmission delay of these calibration signal and their difference can

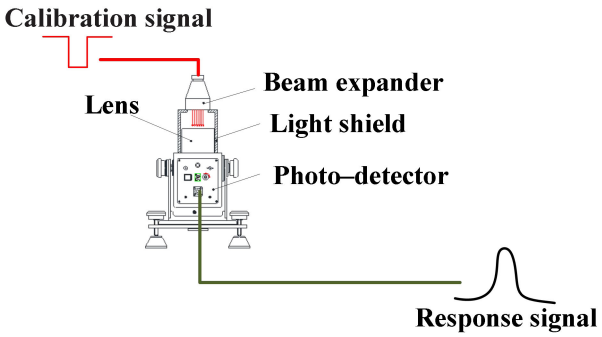

FIGURE 11. Schematic diagram of the calibrated photo-detector.

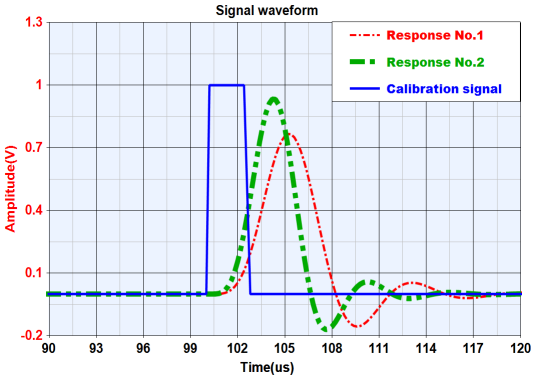

FIGURE 12. Calibration signal vs. two response signals of the measurement channels.

be completely ignored due to relatively short transmission distance. The two ends of the single mode optical fiber are connected into the passive light splitter and beam expander, respectively. This ensures that the calibration signal with the larger diameter of the light beam can project into the lens of the photo-detector, and the photosensitive surface of the light sensor can be utilized as much as possible. Besides, a light shield is added on the lens of the lens of the photo-detector to avoid some interference light. In this way, only the calibration signal projects into the lens as shown in Fig.11.

B. CALIBRATION RESULT

As was stated already, the key indicators of the calibration signal should be properly determined before calibration. In the system, the response time of the photo-detector is 50ns, and its sampling rate is 5MHz. Because sampling interval time is the reciprocal of sampling rate, its sampling interval time is 0.2μs. According to (2), the minimal time-width of the calibration signal is 0.4μs. However, it is difficulty to observe the waveform of the calibration signal and its response signal due to very narrow time-width. In the AWG, we thus determine main indicators of the calibration signal as follows. Its pulse width and edge time are 2.5μs and 10ns, respectively. In the HPTL, the wavelength of the calibration signal can be 665nm according to the performance index of the photo-detector. Obviously, it is in the spectrum of visible light. Besides, the intensity of the calibration signal should be adjusted until it is proper. This means that it cannot bring about the saturation or breakdown of the photo-detector.

For the above system with two measurement channels, we adopt the proposed calibration method in Section III for the corresponding two measurement channels, respectively. Based on the above selected indicators, the experiment platform can generate two parallel calibration signals to output into the calibrated measurement channels. Subsequently, two response signals are generated, as shown in Fig. 12. Due to higher performance, the AWG can generate high- quality calibration signal with little noise. Under the higher SNR, we should use the method based on -3 dB amplitude along drop edge to obtain the arrival time parameter. Through calculation for the two parallel calibration signals, their arrival time parameters are all 102.6μs. Likewise, we calculate the two arrival time parameters of their corresponding response signals, respectively. The arrival time parameter of response signal No.1 is 107.2μs, and that of response signal No.2 is 105.8μs. If they have well equilibrium transmission characteristic, their delay time parameters should be consistent. Unfortunately, there is the difference between them in engineering. In the example, the difference is 1.4μs. Obviously, we must effectively equalize the above difference between any two measurement channels in the research.

According to the proposed method in Section IV, the measurement channel No.1 should be selected as the reference channel by comparison with the two-above calibration.

C. EQUALIZATION RESULT

Based on the above calibration result, an equalization can be performed using the proposed method in Section IV. In the equalization model, it is the core issue that how to construct the compensating network. In essence, we want to acquire the optimized coefficient vector of N tap weights through iteration. Only in this way can this compensating network equalize the non-equilibrium transmission characteristic of the compensated channel.

Firstly, the parameter of $\boldsymbol{w}(N)$ should be initialized. N tap weights are generated, and they obey normal distribution (i.e., the mean of 0 and standard deviation of 1). Besides, the step - size of λ can be determined as 0.02 according to the experience.

Next, the equalization is performed through iteration. We can observe that the waveform of the response signal No.2 changes as the increase of iteration; especially, the difference between the two signals is smaller as shown in Fig. 13.

When iterations are 100, 200, 300 and 400, their corresponding errors are 1μs, 0.8μs, 0.6μs and 0.2μs, respectively. Not until the error is less than 0.5μs do the equalization stop. Under this condition, this can be deemed that the two measurement channels are equilibrium. Consequently, this factor cannot basically affect the estimation accuracy of arrival time parameter. Likewise, for several measurement channels, we can also use the proposed equalization method; that is, except for the reference channel, remaining measurement channels are equalized, respectively.

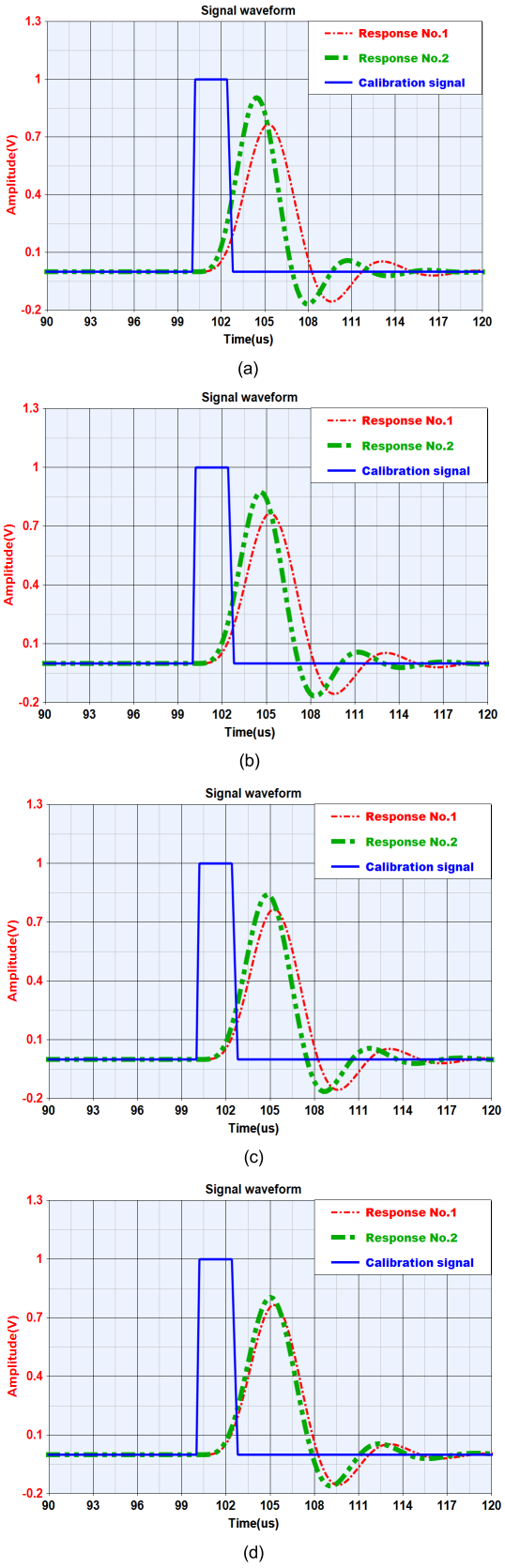

FIGURE 13. Equalization results after iterations, (a) iterations is 100, (a) iterations is 200, (b) iterations is 300, (c) iterations is 400.

Because of simplicity, we adopt the equalization method based on LMS. In the article, it only provides an inspiration for readers. In fact, more other methods, such as Kalman filtering, Particle swarm algorithm, back propagation neural network, can be also effectively used in the equalization.

VI. CONCLUSION

In the article, we propose a novel calibration and equalization method to effectively avoid that non-equilibrium transmission characteristic affects the accuracy of the photoelectric testing system. Based on its measurement principle, the transmission characteristic of the measurement channel is analyzed, and this explains that measurement channels with uniform transmission delay cannot lead to the estimation error of arrival time parameter. According to related requirements of the calibration signal, an experimental platform is developed to generate parallel calibration signals. Due to know signal parameters, we can accurately obtain the transmission delay of every measurement channel; thereby, a measurement channel with maximum transmission delay is determined as the reference channel. Furthermore, we propose an effective method to equalize these measurement channels with on-equilibrium transmission characteristic. Finally, they have nearly same uniform transmission delay, and the error between any two channels is below 0.5μs. Therefore, this factor can be negligible, and it does not affect the measurement accuracy of the system. The proposed calibration and equalization method used in this research is not only limited to the photoelectric testing system, but the possibility also exists to extend the methods used in numerous other photoelectric measurement areas. In future research, we will focus on expanding and generalizing this method to the calibration and equalization for the measurement performance of lidar system, and further research is under discussion.

REFERENCES

[1] N. A. Kazarinov, V. A. Bratov, and N. F. Morozov, "Experimental and numerical analysis of PMMA impact fracture," *Int. J. Impact Eng.*, vol. 143, May 2020, Art. no. 103597.

[2] B. Holfeld, F. Maier, M. Izzo, and S. Dinardo, "Spatial high-speed-imaging of projectile impacts into fluids in microgravity," *Microgr. Sci. Technol.*, vol. 21, nos. 1–2, pp. 73–77, Aug. 2008.

[3] B. D. Buckner and D. L. Esperance, "Digital synchroballistic Schlieren camera for high-speed photography of bullets and rocket sleds," *Opt. Eng.*, vol. 52, no. 8, Aug. 2013, Art. no. 083105.

[4] H. Li, Z. Lei, Z. Wang, and J. Gao, "Research object photoelectric characteristic and fire coordinate distributing probability in across screen system," *J. Nanoelectron. Optoelectron.*, vol. 7, no. 2, pp. 199–203, Mar. 2012.

[5] H. Li, "Research on a new photoelectric detection method to anti-muzzle's flame or light disturbance and projectile's information recognition in photoelectric detection target," *Optelectron. Adv. Mater.-Rapid Commun.*, vol. 8, nos. 7–8, pp. 653–658, 2014.

[6] T. Dong, F. Gao, D. Chen, and J. Yang, "Recognition method of the dual-objective in a linear array CCD-based improved photoelectric measurement system using two lasers with different wavelengths," *Optik*, vol. 217, Sep. 2020, Art. no. 164857.

[7] F. Bing and S. Xiuhua, "Studies of acoustic target with two equilateral triangle arrays," *J. Appl. Acoust.*, vol. 2, pp. 62–66, Mar. 2012.

[8] D. Y. Liu, "Testing system for projectile impact-points based on acoustic sensor network," *J. Ballistics*, vol. 29, no. 2, pp. 85–89. Jun. 2017.

[9] Y. Li, Y. Wang, B. Liu, S. Zhang, and L. Nie, "A new motion parameter estimation and relocation scheme for airborne three-channel CSSAR-GMTI systems," *IEEE Trans. Geosci. Remote Sens.*, vol. 57, no. 6, pp. 4107–4120, Jun. 2019.
[10] L. Gilson, A. Imad, L. Rabet, J. Van Roey, and J. Gallant, "Real-time measurement of projectile velocity in a ballistic fabric with a high-frequency Doppler radar," *Exp. Mech.*, pp. 1–15, Nov. 2020.
[11] W. Ma, T. Dong, H. Tian, and J. Ni, "Line-scan CCD camera calibration in 2D coordinate measurement," *Optik*, vol. 125, no. 17, pp. 4795–4798, Sep. 2014.
[12] T. Dong, D. Hua, Y. Li, and J. Ni, "Measuring principle of vertical target density based on single linear array CCD camera," *Optik*, vol. 125, pp. 176–178, Jan. 2014.
[13] Z. Wu, J. Ni, X. Zhang, and Y. Wu, "Study on verification device of screen spatial location parameters of sky screen target," *Optik*, vol. 125, no. 14, pp. 3770–3773, Jul. 2014.
[14] R. Chen and J. Ni, "Calibration method of light-screen plane equation of sky screen vertical target," *Optik*, vol. 155, pp. 276–284, Feb. 2018.
[15] R. Chen, D. Chen, B. Ji, and J. Ni, "Inversion method of the key structure parameters of light screen array measurement system using genetic algorithm," *Optik*, vol. 206, Mar. 2020, Art. no. 164064.
[16] H. Tian, N. I. Jin-Ping, and J. Ming-Xing, "Moment acquisition algorithm of a projectile passing through a trapezoidal screen," *Acta Photonica Sinica*, vol. 43, no. 12, pp. 114–118, Jul. 2014.
[17] H. Dong, J. Ni, T. Wang, "Research of the information detecte acquire method which the projectile flying the target based on sky screen target," *Nucl. Electron. Detection Technol.*, vol. 29, no. 4, pp. 844–848, Jul. 2009.
[18] H. S. Li and Z. Y. Lei, "Time calculation method base on wavelet analysis in vertical target measurement system," *Infr. Laser Eng.*, vol. 40, no. 9, pp. 1774–1778, Sep. 2011.
[19] D. Chen and J. Ni, "Pulse compression-based improvement on the estimation accuracy of time interval between two trigger signals in light screen array," *Optik*, vol. 158, pp. 675–683, Apr. 2018.
[20] J. P. Ni, "Projectile hitting coordinate using light screen array," in *Technology and Application of Measurement of the Light Screen Array*. Beijing, China: Nat. Defense Ind. Press, 2012, pp. 145–192.
[21] J. Zu et el, "Calibration technology based on new concept dynamic test," in *New Concept Dynamic Test*. Beijing, China: Nat. Defense Ind. Press, 2016, pp. 94–132.
[22] *Verification Method for Sky Screen*, Military Standards Committee of China, Beijing, China, 2017.
[23] *Specification for Sky Screen*, Military Standards Committee of China, Beijing, China, 2017.

DING CHEN (Member, IEEE) was born in Xi'an, Shaanxi, China, in 1982. He received the B.S. degree in electrical & information engineering from the Xi'an Institute of Technology, Shaanxi, China, in 2004, and the M.S. degree in weapon systems and utilization engineering and the Ph.D. degree in optical engineering from Xi'an Technological University (XATU), Shaanxi, China, in 2006 and 2020, respectively.

From 2004 to 2006, he was an Assistant Engineer with Xi'an North Electro-Optic Company, Ltd. From 2009 to 2010, he was a Lecturer with the Electrical & Information Department, Xi'an University of Technological Information. From 2010 to 2016, he was a Senior Engineer with the Radar Design & Research Institute, Xi'an Huang-He Electromechanical Company, Ltd. Since 2020, he has been an Assistant Professor with the School of Armament Science & Technology, XATU. He has authored more than 70 articles in Chinese or English. His research interests include photoelectric measurement & instrument technology, photoelectric information processing & acquisition and radar system design, and simulation and test.

Dr. Chen is a Senior Member of the Chinese Institute of Electronics (CIE) and also a member of SPIE, IET, and IEICE. He attended the 2018 IEEE International Conference on Mechatronics and Automation (ICMA 2018) and the 2018 IEEE International Conference on Sensor Networks and Signal Processing (SNSP 2018), in Changchun and Xi'an, China, respectively. Specially, he made an oral presentation in the ICMA 2018, and a poster was shown in the SNSP 2018. Besides, his two articles were published in the PROCEEDINGS OF THE IEEE of the two above international conferences. Besides, he is a Reviewer of *IET Signal Processing*, the *American Journal of Information Science & Technology*, the *Romania Journal of Optoelectronics & Advanced Materials*, and the *Chinese Journal of Ordnance Equipment Engineering*.

JINPING NI was born in Qian, Shaanxi, China, in 1965. He received the B.S. degree in industrial electrical automation from the Xi'an Institute of Technology (XIT), Shaanxi, China, in 1985, the M.S. degree in theory and application of automatic control from the Beijing Institute of Technology, Beijing, China, in 1993, and the Ph.D. degree in weapon systems and utilization engineering from Northwestern Polytechnical University, Shaanxi, China, in 2002.

From 1985 to 1980, he was an Assistant Engineer with the Scientific Research Institute, XIT. From 1993 to 1994, he was an Engineer and the Deputy Director of the Photoelectric Testing Technique Institute, XIT. From 1994 to 1998, he was a Senior Engineer, a Master's Supervisor, and the Deputy Director of the Photoelectric Testing Technique Institute, XIT. From 1998 to 2003, he was a Professor, a Master's Supervisor, and the Director of the Photoelectric Testing Technique Institute, XIT. From 2003 to 2015, he was a Professor, a Doctoral Supervisor, and the Dean of the School of Optoelectronic Engineering and also the Executive Deputy Director of the Shaanxi Province Key Laboratory of Photoelectric Measurement and Instrument Technology, Xi'an Technological University (XATU). From 2016 to 2019, he was a Professor, a Doctoral Supervisor, and the Dean of the Graduate School and the Executive Deputy Director of the Shaanxi Province Key Laboratory of Photoelectric Measurement and Instrument Technology, XATU. Since 2019, he has been a Professor, a Doctoral Supervisor, and the Dean of the School of Mechatronic Engineering and has also been the Executive Deputy Director of the Shaanxi Province Key Laboratory of Photoelectric Measurement and Instrument Technology, XATU. He has authored more than 100 articles in Chinese or English. His research interests include photoelectric measurement & instrument technology, photoelectric information processing & acquisition and weapon system measurement & testing. Besides, he is a member of editorial board the *China Journal of Applied Optics*.

Dr. Ni is a Senior Member of the China Ordnance Society, and he is also a member of the Chinese Optical Society and the Chinese Society of Aerospace.